Astronomy & Astrophysics

SDSS photometry of asteroids in cometary orbits
(Research Note)

A. Alvarez-Candal[1,2]

[1] ESO, Alonso de Córdova 3107, Vitacura, Casilla 19001, Santiago 19, Chile
e-mail: `aalvarez@eso.org`
[2] Instituto de Astrofísica de Andalucía, CSIC, Glorieta de la Astronomía s/n, 18008 Granada, Spain

ABSTRACT

Aims. Aiming at exploring the relationship between asteroids in cometary orbits and other minor body populations from the observational point of view, I explore the large photometric database of the Sloan Digital Sky Survey – Moving Objects Catalog.
Methods. The sample of interest was carefully selected by analyzing colors and orbital properties within the data in the catalog. I computed the spectral slope for each object and compared with published spectroscopic results of other asteroids in cometary orbits, as well as with other populations of asteroids in the outer region of the main belt and Trojans.
Results. Using this extended database I find that asteroids in cometary orbits with Tisserand parameter below 2.9, and especially below 2.8, are most likely of primitive origin. The population of objects with Tisserand parameter larger than 2.9 is a mixture of populations ranging from the inner to the outer main belt.

Key words. catalogs – minor planets, asteroids: general

1. Introduction

An "asteroid in cometary orbit" (ACO) is an asteroid-like (no apparent coma) object in a cometary-like orbit. Classically a cometary orbit has $T_J < 3$, where T_J is the Tisserand parameter with respect to Jupiter and is given by

$$T_J = a_J/a + 2 \cos I \sqrt{(a/a_J)(1 - e^2)}, \qquad (1)$$

where a, e, I are the usual orbital elements of the asteroid, and a_J is the semi-major axis of Jupiter. Asteroids in the main belt have usually $T_J > 3$ (Kresák 1979).

The parameter T_J is a constant of motion in the frame of the restricted three body problem where the reference plane is that of Jupiter, therefore the inclination must be referred to that of the Jovian planet. By definition ACOs have orbits with moderate to high inclinations and eccentricities and have low relative speed encounters with Jupiter, thus it is an unstable population, just like comets from the Jupiter family, JFCs, that have dynamical lifetimes of $\sim 10^5$ yr (see, for instance, Alvarez-Candal & Roig 2005). That we can observe them indicates that the population must be replenished from one or several sources. The most probable are asteroids from the main belt (I consider those between 1.8 and 3.2 AU), the populations beyond the outer part of the main belt: Cybele ($\sim$3.4 AU), Hilda ($\sim$3.9 AU), Trojan asteroids ($\sim$5.2 AU), and JFCs. These last four populations will be collectively called "primitive" objects for simplicity. Here I use the word primitive with a wide meaning as those minor bodies whose interiors have not been widely thermally processed, are likely to have a surface (or subsurface) content of water ice, and have perhaps undergone water alteration (see Chaps. 5, 8, and 9 from de Pater and Lissauer 2007).

The present Research Note is an extension of a work by Licandro et al. (2008, hereafter L08). They found that the spectra of ACOs from the visible up to the near-infrared are like those of Hilda or Trojan asteroids, but they could not set stringent constraints on the possible dynamical source of ACOs. Nevertheless, they propose that ACOs with $T_J \sim 3$ are composed of a mix of bona fide asteroids and primitive objects, while more primitive objects are found when going to $T_J < 2.9$. I extend their work using a larger database provided by the data from the fourth release of the Sloan Digital Sky Survey – Moving Objects Catalog (MOC) aiming at a better comparison with other primitive populations. In the next section I discuss how to define the sample of ACOs, while in Sect. 3 the results are presented which are then discussed in Sect. 4.

2. Sloan digital sky survey: defining the sample

The Sloan digital sky survey is a large photometric survey developed mainly for stellar and extragalactic astronomy. It consists of a set of five magnitudes: $m_{u'}$, $m_{g'}$, $m_{r'}$, $m_{i'}$, and $m_{z'}$. As a by-product of the reduction pipeline, candidates for moving objects are flagged (Ivezić et al. 2001) and are included in the MOC. It is then possible to associate these data to real asteroids (Jurić et al. 2002). There are more than 100 000 identified asteroids in the MOC, representing almost 50 times more objects that the spectroscopic database, slightly over 2000 spectra combining the SMASS (Bus & Binzel 2002) and S^3OS^2 (Lazzaro et al. 2004) databases.

To define the sample of ACOs I selected from the fourth MOC release all observations linked to objects with $T_J \leq 3.02$, discarding Centaurs, Trojan, Hilda, and Cybele asteroids (as in Alvarez-Candal & Licandro 2006 and L08). After this first selection criterion a total of 666 observations remained. The upper cut-off in Tisserand parameter is the current value of T_J of the JFC 2P/Encke.

The second step in the selection was based on the relative reflectance computed from the Sloan magnitudes. They are defined

Table 1. ACOs with Sloan and spectroscopic data.

Object	S' (% $(0.1\,\mu m)^{-1}$) Spec.[a]	S' (% $(0.1\,\mu m)^{-1}$) This work
(6144) 1994 EQ$_3$	7.45	9.81
(19748) 2000 BD$_5$	5.16	1.01

References. [a] Licandro et al. (2008).

on a set of five filters: u', g', r', i', z', centered at 0.354, 0.477, 0.623, 0.763, and 0.913 μm, respectively. The reflectances are computed using

$$F_j = 10^{-0.4[(m_j - m_{r'}) - (m_j - m_{r'})_\odot]}, \qquad (2)$$

where m_j and $m_{r'}$ are the magnitudes in the j and r' filters, while $\odot$ represents the solar colors (from Ivezić et al. 2001). The reflectance is normalized to unity at the central wavelength of the r' filter, and they represent a very low-resolution spectrum. The normalization was chosen to make the database compatible with previous works (such as Roig et al. 2008).

Using the computed values of reflectance, I eliminated all objects with relative errors greater than 10%, in g', r', i', or z'. Anomalous values of flux were also discarded, i.e., $F_{g'} > 1.3$, $F_{i'} > 1.5$, $F_{z'} > 1.7$, or $F_{g'} < 0.6$ (see Roig & Gil-Hutton 2006). The sample was then reduced to 302 measurements, including some objects with more that one observation.

In the final step, I inspected all the remaining reflectances by eye, eliminating those objects with behavior similar to S- or V-type asteroids (73 objects, generically called "with bands"). I also eliminated those objects with unrealistic reflectance that survived the previous step. The sample was reduced to 111 observations of 94 objects.

Finally, I computed the spectral slope S' by means of a linear fit to the fluxes F_j, discarding the u' flux, taking the errors in each flux into account. The spectral slope is a measure of the redness of the spectrum: the higher the value the redder the spectrum. For those objects with more than one observation, S' was computed as the weighed mean of each individual value of S'. The final sample includes 94 objects with spectral reflectance that resemble those of featureless spectra (such as B-, C-, X-, or D-type asteroids).

3. Results

I compared the list of 94 ACOs with the spectroscopic sample presented in L08. There are two objects in common: (6144) 1994 EQ$_3$ and (19748) 2000 BD$_5$, and the comparison of the spectral slopes is given in Table 1. Considering that error bars of the slopes are typically about 2% $(0.1\,\mu m)^{-1}$, the values in Table 1 are consistent.

In L08 a relationship was found between T_J and S' among the ACOs. Objects with low values of T_J tend to have the reddest slopes. The spectroscopic database presented in their work included 32 featureless ACOs, while now I have a sample that is three times larger. Figure 1 shows the Sloan data and the spectroscopic data in the $S' - T_J$ space. In order to compare the values of S' of both dataset, I recomputed the slopes of L08 by renormalizing them to 0.623 μm, which is the central wavelength of the r' filter.

The Sloan slopes follow the same pattern as detected with the spectroscopic data, therefore confirming the results presented in L08. Nevertheless, among the Sloan data there are a few objects
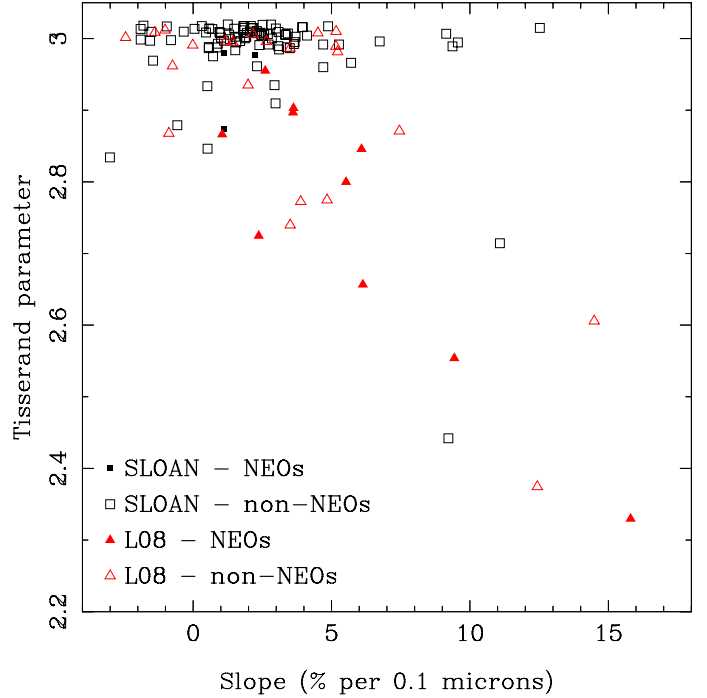
Fig. 1. Spectral slope vs. T_J. Squares represent ACOs from Sloan, while triangles represent ACOs from L08. Filled symbols indicate objects in near Earth orbits. In the plot the only represented objects are those classified as featureless, see text.

with red colors ($\sim$10% $(0.1\,\mu m)^{-1}$) and $T_J \sim 3$, which were not seen in L08. Also, among the new data, there are no objects as red as the reddest in L08. I do not find any object with $T_J < 2.8$ and neutral-blue slopes. I tested the apparent correlation seen using the Spearman rank-order correlation test (Press et al. 1992). The test relies on no parameter or a priori hypothesis. It computes the correlation coefficient r and its reliability by means of P_r. The result gives $r = -0.27$, $P_r = 99.8\%$, i.e., the anti-correlation seen is statistically reliable over 3 sigma.

I also explored other possible correlations using orbital parameters (Figs. 2 and 3). The most significant one is found between spectral slope and eccentricity $r = 0.18$ with a reliability over 2 sigma, which is most likely related to the strong correlation found above through the Tisserand parameter (Eq. (1)).

A comparison of the distribution of spectral slopes, spectroscopic and Sloan, is seen in Fig. 4. The distributions span about the same range of slopes, with two objects in the spectroscopic database redder than any ACO from the Sloan database.
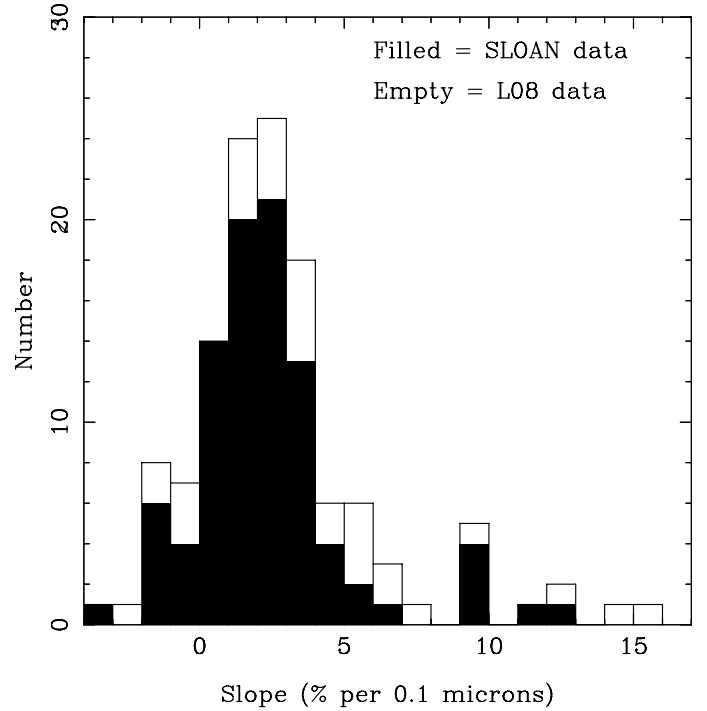
Three works study primitive populations of the solar system using Sloan photometry: Gil-Hutton & Brunini (2008), Roig et al. (2008), and Gil-Hutton & Licandro (2010) studying the Hilda, Trojan, and Cybele asteroids, respectively. I compare the distribution of spectral slopes for the three samples in Fig. 5.

The distributions are different, spanning more or less the same range of slopes. The ACOs have a majority of objects with slopes 0–5% $(0.1\,\mu m)^{-1}$, which, according to Fig. 1 have $T_J \sim 3$. Nevertheless, there is a tail of objects with $S' \geq 10$, which coincides with the reddest objects from the other populations.
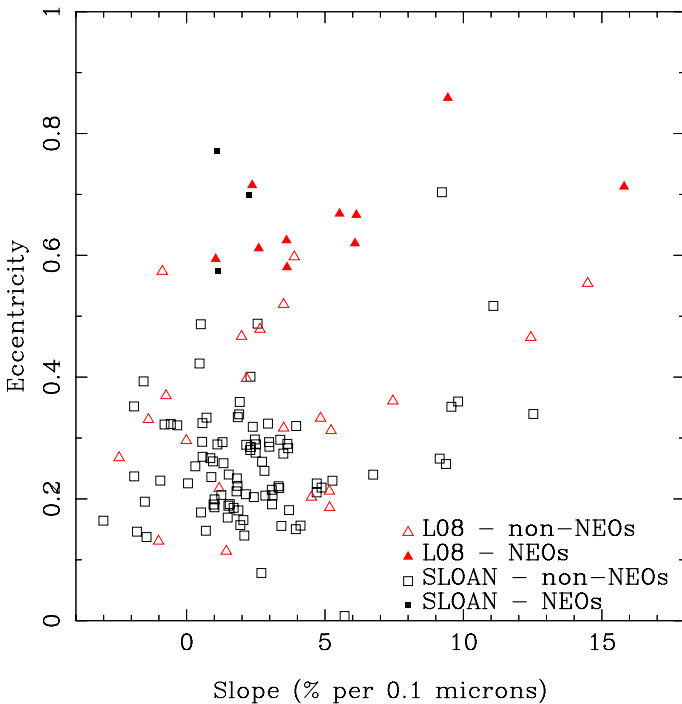
I ran a Kolmogorov-Smirnov test (Press et al. 1992) to compare the ACOs slope distribution with each one of the other three distributions presented in Fig. 5 and to test the null hypothesis that they have been extracted from the same parent distribution. The results came out negative in each case.
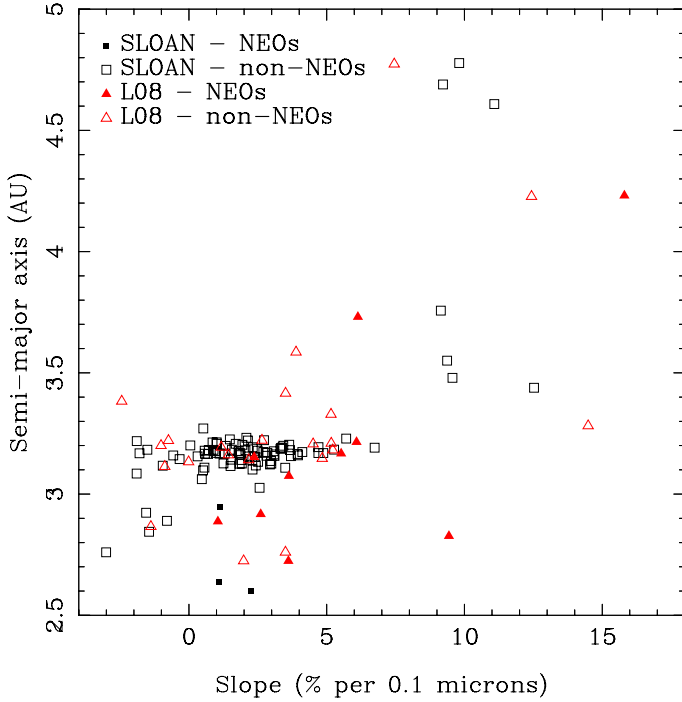
Fig. 2. Spectral slope vs. semi-major axis. The symbol convention is the same as in Fig. 1.
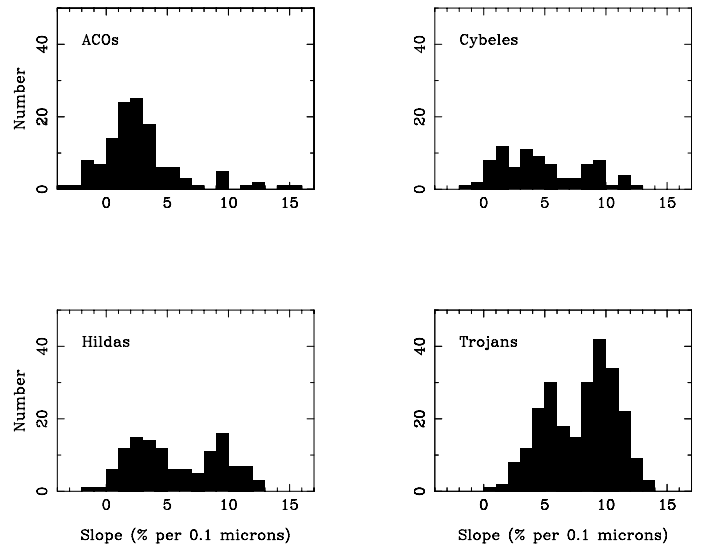

Fig. 3. Spectral slope vs. eccentricity. The symbol convention is the same as in Fig. 1.

Fig. 4. Distribution of spectral slopes for the ACOs. The chosen bin is 2% $(0.1\,\mu m)^{-1}$.

Fig. 5. Distribution of spectral slopes for the four different populations. *Top left*: ACOs, this work plus those from L08; *Top right*: Cybele asteroids from Gil-Hutton & Licandro (2010); *Bottom left*: Hilda asteroids from Gil-Hutton & Brunini (2008); *Bottom right*: Trojan asteroids from Roig et al. (2008). The chosen bin is 2% $(0.1\,\mu m)^{-1}$.

4. Discussion

Using the Sloan digital sky survey data I increased the number of ACOs with physical observations by a factor three pushing the limiting magnitude of detection by one (see Fig. 6). This only applies to ACOs in non-NEO orbits. Figure 6 should be regarded as illustrative of gain in number by using the Sloan database. Nevertheless, it should be kept in mind that the sample is affected by at least two selection effects. The first one is a bias

against near-Earth objects (NEOs): by observational strategy an object must be observed with all five filters to be flagged as a moving object candidate, which is not the case for near-Earth orbits that have high speed and cross the field-of-view faster than the rate at which the telescope switches filters. The second one is against the farther, darker, smaller objects.

The slope distribution of ACOs could reflect the distributions from the contributing populations. Dynamical studies indicate that Trojan and Hilda asteroids could contribute to the population of asteroids in cometary orbits (Levison et al. 1997; Di Sisto et al. 2005). As the ACO distribution of slopes does not resemble
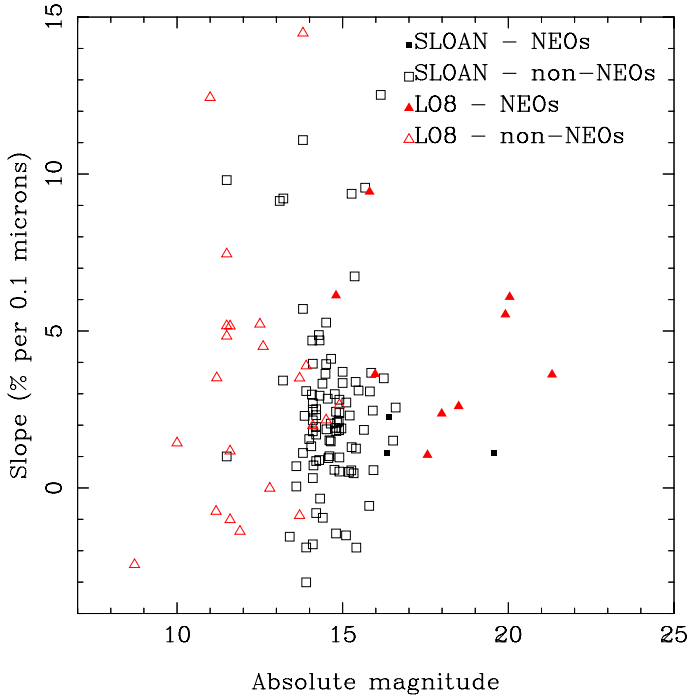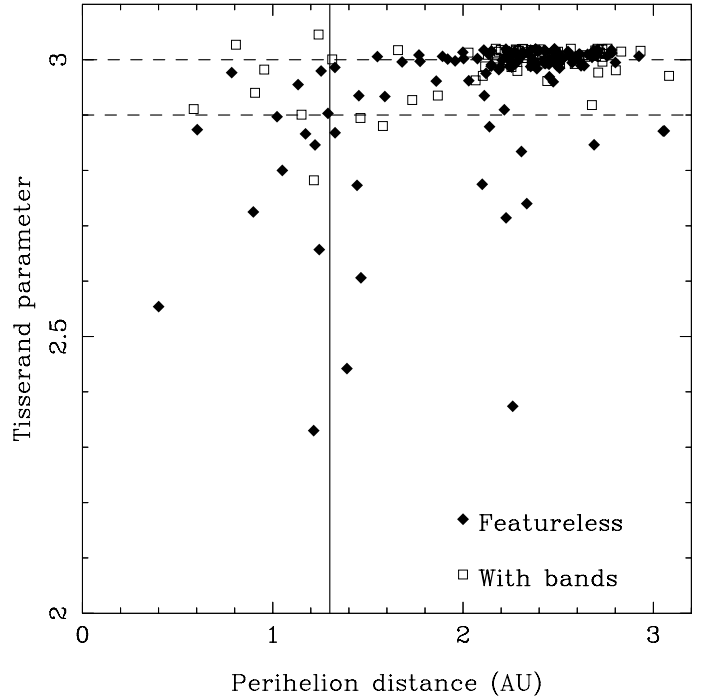
Fig. 6. Absolute magnitude vs. spectral slope for the ACOs' samples. The symbol code is the same as that in Fig. 1.

Fig. 7. Perihelion distance vs. Tisserand parameter. The open squares indicate ACOs with bands. Filled rhombuses indicate featureless ACOs. The continuous line separates the NEOs ($q < 1.3$ AU) from the non-NEOs. Dashed horizontal lines indicate $T_J = 2.9$ and $T_J = 3.0$. All ACOs from L08 and this work are considered together.

those of Cybele, Hilda, or Trojan asteroids (Fig. 5), they are not the only contributors, probably not even the main ones, therefore the main belt or JFCs are probably important, too. Figure 2 shows that most of the ACOs with neutral or slightly red spectral slopes (C or X taxonomical classes) are located just below 3.2 AU, the outer limit of the main belt. These objects are also located mostly around $T_J \sim 3$, and probably have their origin within the main belt.

As a byproduct of the distributions of slopes, we can see that there is an increase in the average value of S' with increasing distances from the Sun: 2.8% $(0.1\,\mu m)^{-1}$, 4.8% $(0.1\,\mu m)^{-1}$, 5.8% $(0.1\,\mu m)^{-1}$, and 8.13% $(0.1\,\mu m)^{-1}$ for ACOs, Cybele, Hilda, and Trojan asteroids, respectively.

Figure 7 reproduces Fig. 3 from L08. It shows all ACOs in the sample: featureless and with bands, as described above. The figure shows that most of the ACOs with bands have $T_J > 2.9$, with very few exceptions. This confirms the result presented in L08 with a smaller database. The population at $T_J \sim 3$ is probably a mix of asteroids from the inner and outer regions of the main belt and a few primitive objects, while at lower values of T_J, there are probably objects that were injected into those orbits from primitive populations. I remind the reader that the convention used in this work calls primitive populations all those outside the main belt, i.e., farther than 3.2 AU, as well as Jupiter family comets.

Considering together the Sloan and L08 samples, and remembering that there are two objects in common, there are observations for a total of 204 ACOs, 124 of which have featureless spectra. In the subpopulation of NEOs there are 21 objects, 14 of which are featureless (67%, in good agreement with the DeMeo & Binzel 2008 estimative). A similar fraction, 60% of the objects, are featureless in the non-NEO population. When considering only objects with $T_J < 2.9$, the fractions change radically, and so does the number of observed ACOs. In all, 24 out of 27 objects are featureless (89%). The fraction of featureless

ACOs is more or less constant for either the NEO (10 out of 11) or non-NEO (14 out of 16) populations.

It is known that the near-Earth region is a mixture of different populations of minor bodies: Main belt and primitive populations (Bottke et al. 2002). When I consider objects that have $T_J < 2.9$ the results indicate a lower contribution from asteroids from the main belt where objects with bands predominate (see Mothé-Diniz et al. 2003).

To the best of my knowledge, no dynamical study has been carried out about the possible origins of the ACOs in non-NEO orbits. Nevertheless, the mix found for $T_J > 2.9$ indicates a mixture of different populations, perhaps similar to what is seen for NEOs. The main belt population of asteroids has typical values of $T_J > 3.0$, thus it still needs to be understood how those objects had their orbits excited to $2.9 < T_J < 3.0$. One possibility is resonant perturbations. Once more, as with the NEOs, objects that have $T_J < 2.9$ had, for the most part, their sources in the primitive populations.

Another open question is what the link is between the ACOs dynamical evolution and the physical-chemical evolution of their surfaces. Figure 7 hints that most of the objects with features in their spectra, which come from the main belt of asteroids, are not able to dynamically evolve to values of $T_J < 2.9$, therefore reinforcing the possibility that the ACOs with $T_J < 2.9$ have their source in the primitive populations.

References

Alvarez-Candal, A., & Licandro, J. 2006, A&A, 458, 1007
Alvarez-Candal, A., & Roig, F. 2005, in Dynamics of Populations of Planetary Systems, eds. Z. Knežević, & A. Milani (Cambridge: Cambridge Univ. Press), 205
Bottke Jr., W. F., Morbidelli, A., Jedicke, R., et al. 2002, Icarus, 156, 399
Bus, S. J., & Binzel, R. P. 2002, Icarus, 158, 106
DeMeo, F. E., & Binzel, R. P. 2008, Icarus, 194, 436
de Pater, I., & Lissauer, J. J. 2007, Planetary Sciences (Cambridge: Cambridge University Press)
Di Sisto, R. P., Brunini, A., Dirani, L. D., et al. 2005, Icarus, 174, 81
Gil-Hutton, R., & Brunini, A. 2008, Icarus, 193, 567
Gil-Hutton, R., & Licandro, J. 2010, Icarus, 206, 729
Ivezić, Ž., Tabachnik, S., Rafikov, R., et al. 2001, AJ, 122, 2749
Jurić, M., Ivezić, Ž., Lupton, R. H., et al. 2002, AJ, 124, 1776
Kresák, L. 1979, in Asteroids, ed. T. Gehrels (Tucson: Univ. Arizona Press), 289
Lazzaro, D., Angeli, C. A., Carvano, J. M., et al. 2004, Icarus, 172, 179
Levison, H. F., Shoemaker, E. M., & Shoemaker, C. S. 1997, Nature, 385, 42
Licandro, J., Alvarez-Candal, A., de León, J., et al. 2008, A&A, 481, 861
Mothé-Diniz, T., Carvano, J. M., & Lazzaro, D. 2003, Icarus, 162, 10
Press, W. H., Teukosky, S. A., Vetterling, W. T., et al. 1992, Numerical Recipes, 2nd edn. (Cambridge: Cambridge University Press)
Roig, F., & Gil-Hutton, R. 2006, Icarus, 183, 411
Roig, F., Ribeiro, A. O., & Gil-Hutton, R. 2008, A&A, 483, 911